

## Lidar analysis

Optimal estimation (OE) retrieval, a form of non-linear regression, has been successfully applied to the analysis of radiometer, radar, and other observations but has not seen substantial use within the lidar community. Two applications to Raman lidar are outlined here — estimation of the overlap function from routine observations [1] and the simultaneous retrieval of aerosol extinction, backscatter, and lidar ratio [2].

These retrievals consider the full profile at once, making optimal use of the information available. The retrieval (in effect) chooses the most appropriate vertical resolution for the results while fully characterising the uncertainty due to measurement noise, model error, and other assumptions.

## Optimal estimation retrieval

As outlined in [3], OE solves the inverse problem,

$$y = F(x, b) + \epsilon,$$

where  $y$  contains the lidar profiles (with noise  $\epsilon$ ). The forward model  $F(x, b)$  translates a state of the atmosphere into a simulated measurement. The state is specified by unknown parameters  $x$  and known parameters  $b$ .

The probability that the system has a state  $x$  given the measurement  $y$  can be written as,

$$[y - F(x, b)]^T S_y^{-1} [y - F(x, b)] + [x - x_a]^T S_a^{-1} [x - x_a],$$

where the covariance matrix  $S_y$  summarises the uncertainty in both the measurement and parameters while  $x_a$  is the a priori state with covariance  $S_a$ . It can be shown that the iteration,

$$x_{i+1} = x_i + [(1 + \Gamma_i) S_a^{-1} + K_i^T S_y^{-1} K_i]^{-1} \{K_i^T S_y^{-1} [y - F(x_i, b)] - S_a^{-1} (x_i - x_a)\},$$

converges to the most probable state  $\hat{x}$ , where the  $K_i = \nabla_{x_i} F(x_i, b)$  and  $\Gamma_i$  is a scaling constant.

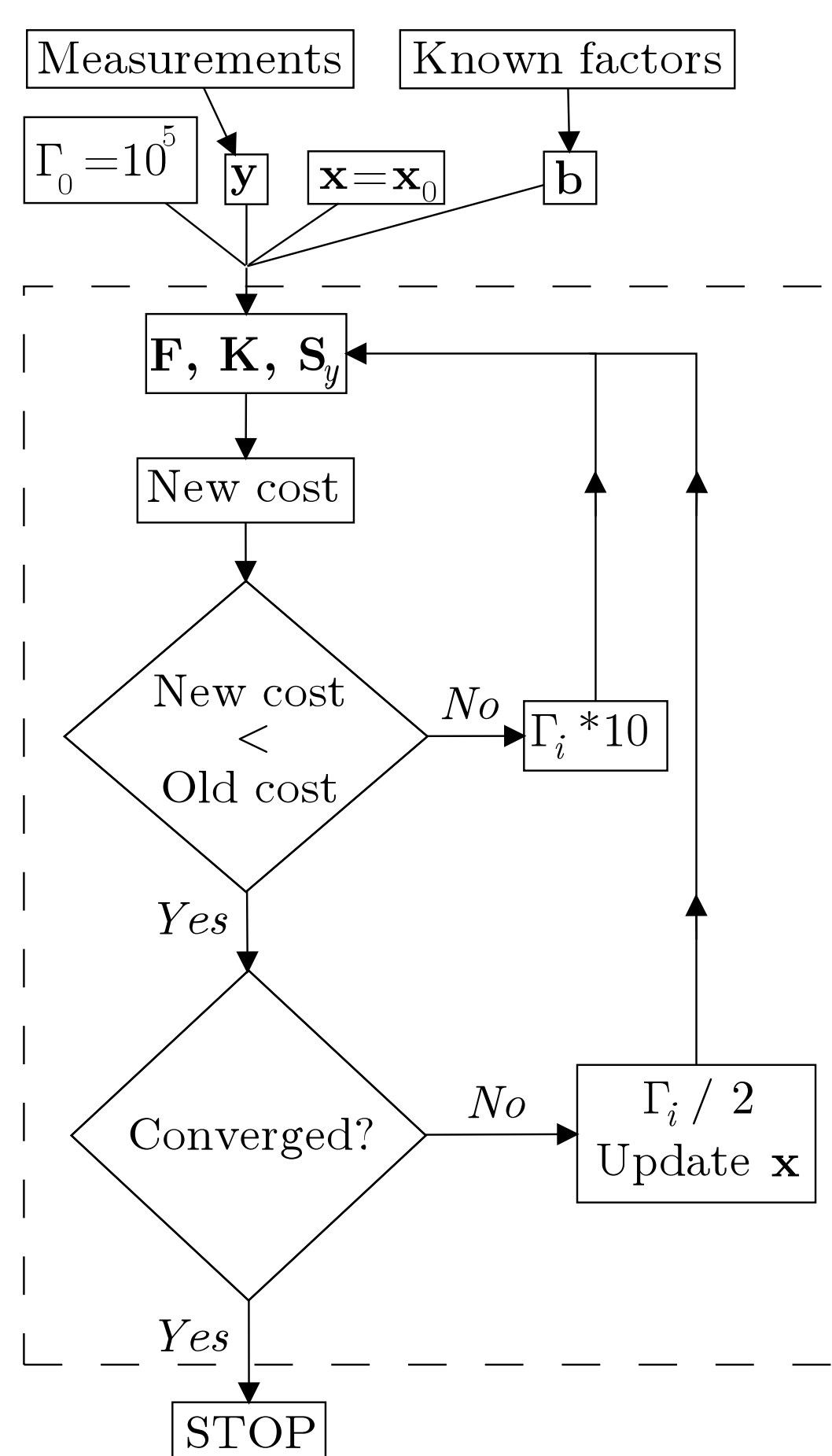


Fig. 1: Schematic of algorithm.

## Estimation of the overlap function

The overlap function of a lidar is the primary source of uncertainty in (roughly) the first kilometre of a lidar profile [4]. Numerous techniques exist to estimate it, but these either require an independent measurement of the aerosol profile or reason to believe it is homogeneous. We developed an OE retrieval of the overlap function [1] from the Raman profile using the traditional lidar equation as a forward model. This fit an analytic formulation of the overlap function outlined in [5] and an error function modelling the aerosol profile. Due to numerous local minima of the cost function and minimal a priori knowledge, the retrieval is annealed (repeated using a random selection of first guesses) to find the optimal solution.

Fig. 2 shows the difference between a variety of simulated overlap functions and that retrieved by this technique, the Raman technique of [6], and a simple analytic inversion assuming a clean atmosphere. The OE retrieval is usually substantially more accurate, even when the noise on the measurements is artificially decreased for the Raman technique. Further, because it retrieves an analytic overlap function, the result is a smooth function, eliminating the artefacts produced by traditional overlap corrections.

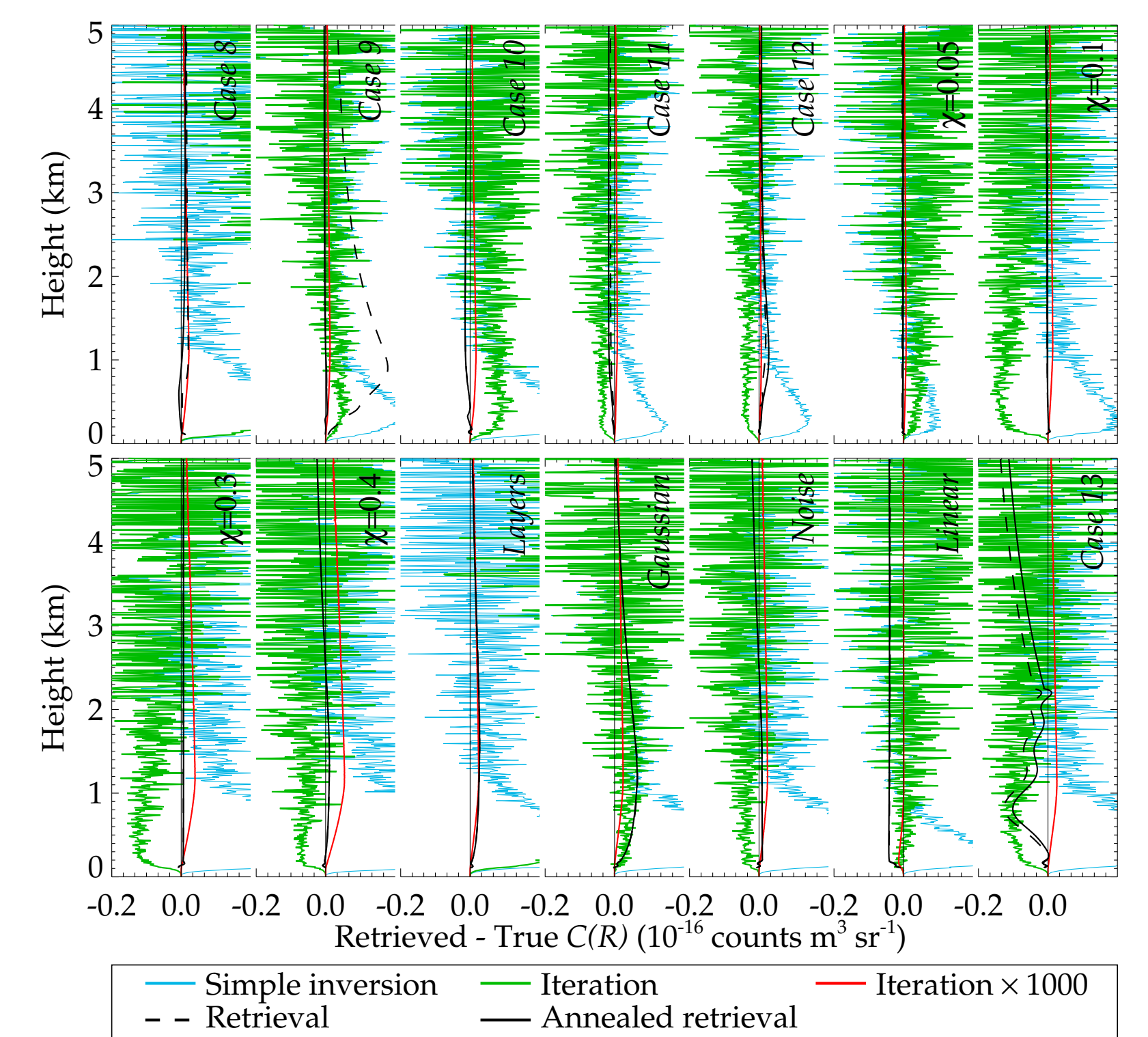


Fig. 2: Error in retrieved overlap function for the OE retrieval (black), traditional Raman technique (green), the same with noise reduced by a factor  $10^3$ , and a simple, analytic technique (blue).

## Extinction, backscatter and lidar ratio

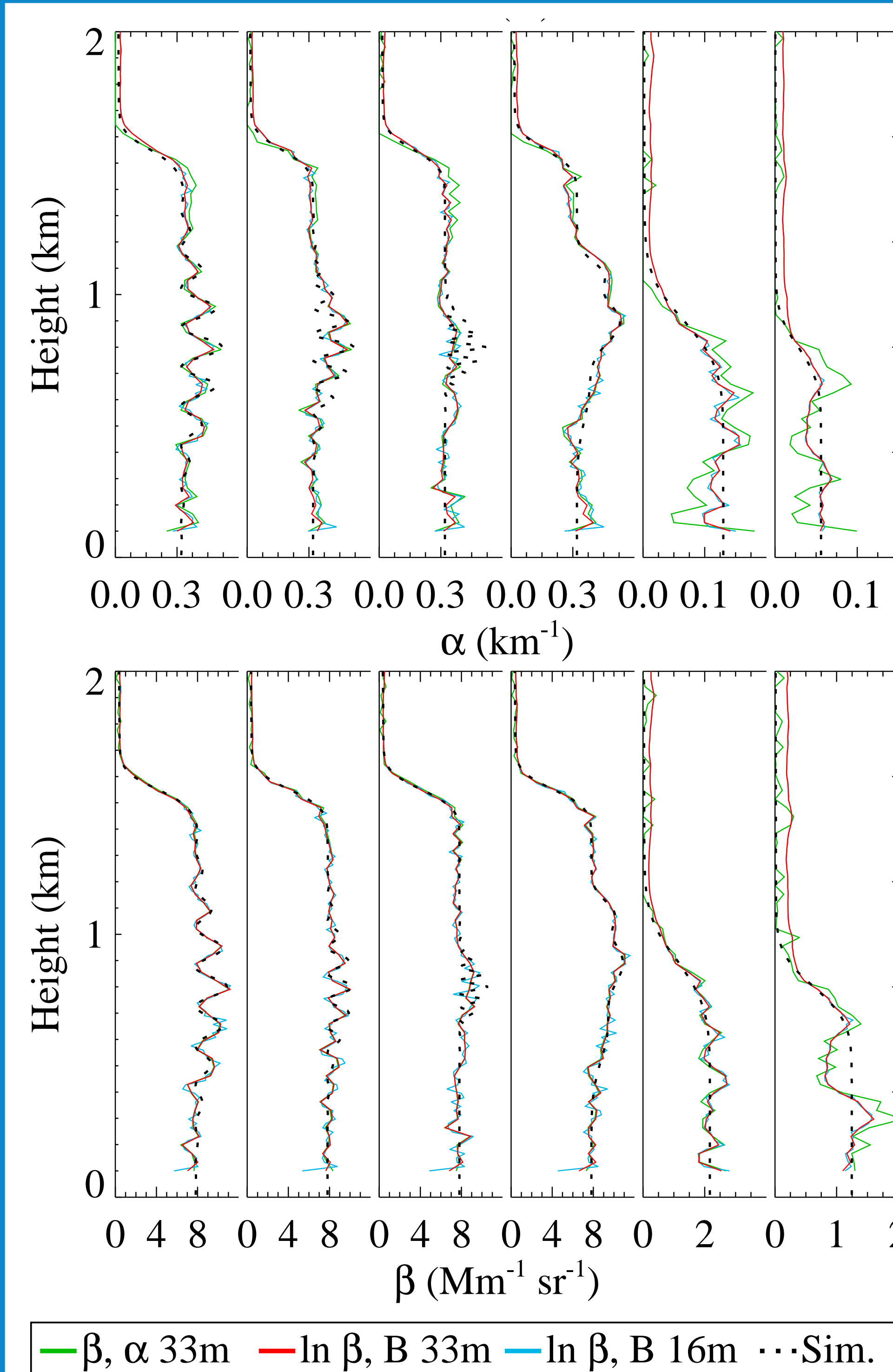


Fig. 3: Retrievals from six simulations (dashed) when retrieving backscatter and extinction (green) or log backscatter and lidar ratio (red at 33 m resolution; blue at 16 m).

Knowing the overlap function, backscatter ( $\beta$ ) and either extinction ( $\alpha$ ) or lidar ratio ( $B$ ) can be retrieved from paired elastic and Raman profiles [2]. Both configurations successfully reproduce simulated data in a variety of circumstances, including complicated layering as shown in Fig. 3. The last two cases shown have decreased SNR, producing noisier results. The retrieval compares favourably to traditional techniques in Fig. 4

The lidar ratio is conceptually easier to constrain with an a priori but is sensitive to both profiles, increasing its reliance on those assumptions. Extinction can be more weakly constrained, but has difficulty with cloud as the backscatter greatly exceeds any useful prescribed range. The resolution of these products can be estimated from the width of the rows of the averaging kernel,  $A = (K^T S_y^{-1} K + S_a^{-1})^{-1} K^T S_y^{-1} K$ . Though the backscatter kernels are virtually delta functions ( $\sim 30$  m resolution), the extinction and lidar ratio kernels have widths of  $\sim 300$  m, which increases in the free troposphere (due to the decreased SNR).

## Comparison to existing techniques

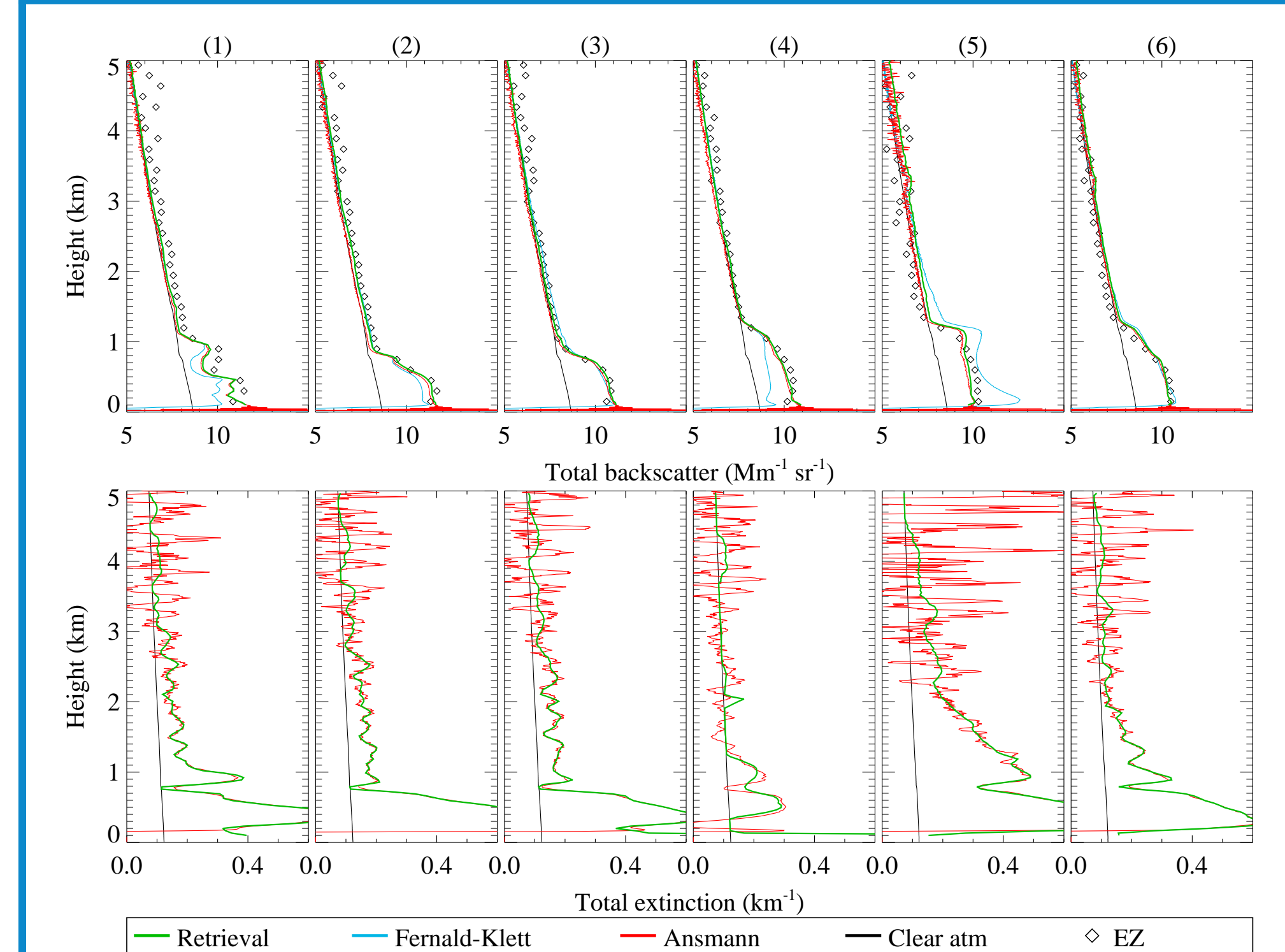


Fig. 4: Total backscatter (top) and two-way extinction (bottom) determined by this retrieval (green), the Fernald-Klett elastic inversion [7] (blue), and the Ansmann Raman technique [8] (red) for six profiles observed during March 2010. The attenuated backscatter coefficient reported by an independent lidar is shown (diamonds) for comparison. The scattering from a clear atmosphere is shown in black, highlighting negative  $\alpha$  returned by the traditional techniques.

## Instrumentation

The results presented here are simulated for or collected by the Robust And Compact Hybrid Environmental Lidar (RACHEL), developed by Hovemere, Ltd. It is a 355 nm coaxial Raman lidar system designed for unattended operation in the field. Constructed from off-the-shelf components, the instrument provides a low-cost platform for pollution monitoring. The prototype suffered significant technical difficulties, severely limiting the quality of the data. As such, we are eager to collaborate with any groups interested in applying these techniques to a research-grade Raman lidar.

## References

- [1] A.C. Povey et al. (2012), doi:10.1364/AO.51.005130.
- [2] A.C. Povey et al. (2014), doi:10.5194/amt-7-757-2014.
- [3] C. Rodgers, *Inverse methods for atmospheric sounding*, World Scientific (2000).
- [4] A.C. Povey (2013), <http://ora.ox.ac.uk/objects/uuid:eb94de02-ad92-4eeb-b15c-094b05fa11c6>.
- [5] T. Halldórsson and J. Langerholc (1978), doi:10.1364/AO.17.000240.
- [6] U. Wandinger and A. Ansmann (2002), doi:10.1364/AO.41.000511.
- [7] J. Klett (1985), doi:10.1364/AO.24.001638.
- [8] A. Ansmann et al. (1992), doi:10.1364/AO.31.007113.

## Retrieval of ash properties

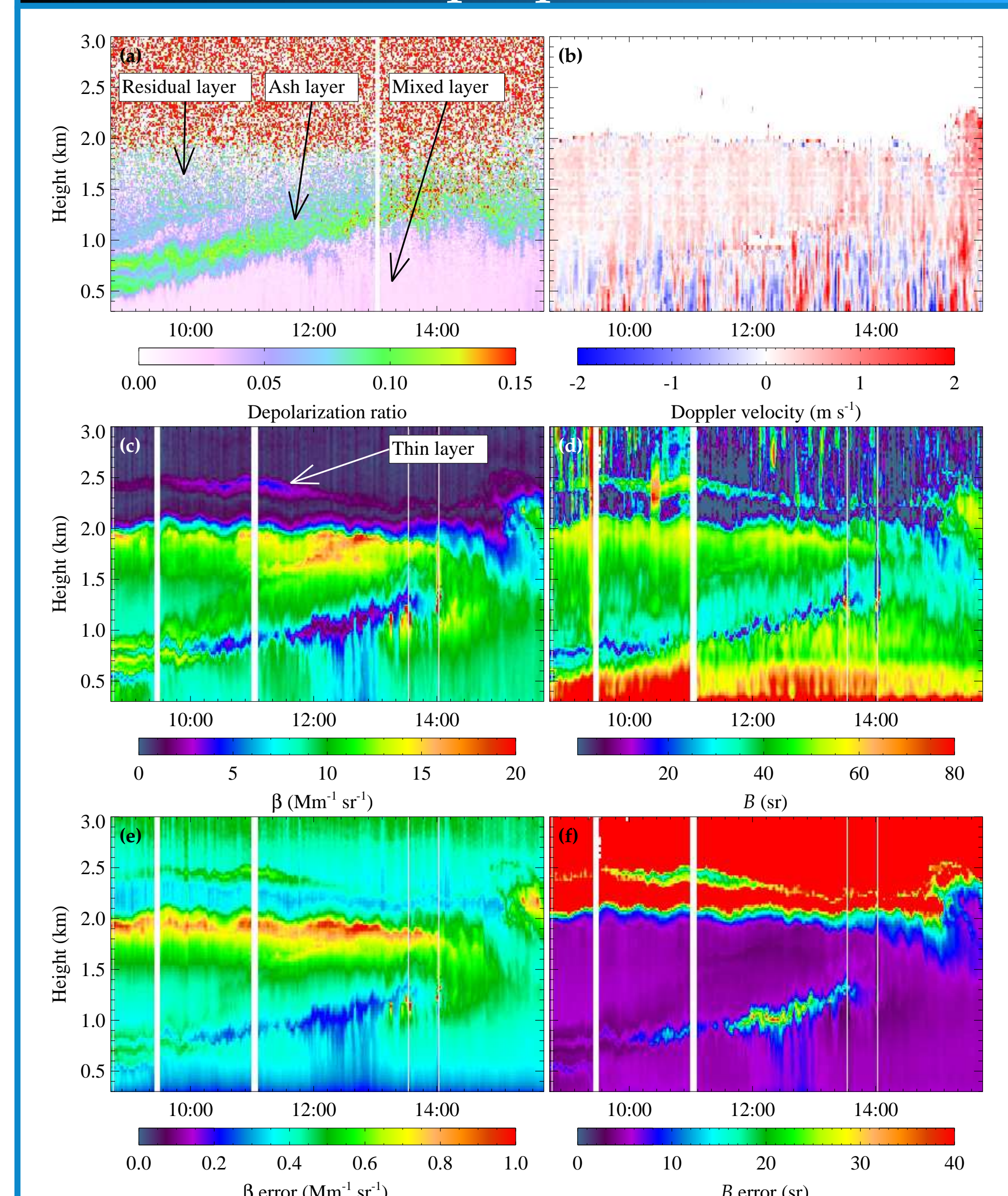


Fig. 5: Observations of the Eyjafjallajökull plume over the UK on 19 April 2010. (a) Depolarization ratio highlighting a layer of ash; (b) Vertical velocity; (c-d) Retrieved backscatter and lidar ratio; (e-f) Uncertainties on (c-d).